

Luminescent coordination polymer gels based on rigid terpyridyl phosphine and Ag(I)<sup>†</sup>

Xin Tan, Xue Chen, Jianyong Zhang\* and Cheng-Yong Su

Received 6th January 2012, Accepted 8th February 2012

DOI: 10.1039/c2dt00035k

**Rigid bridging terpyridyl phosphine and AgOTf form nanofibres to induce gelation of organic solvents, and the gel emits blue luminescence by suppressing  $\pi$ - $\pi$  interactions between ligands.**

Supramolecular gels are self-assembled through non-covalent intermolecular interactions including van der Waals,  $\pi$ - $\pi$  stacking, hydrogen bonding, and/or hydrophobic effects. Discrete metallomolecules or coordination polymers are found to be gelators through non-covalent interactions including metal-ligand coordination.<sup>1</sup> Due to incorporation of metals, metalogels have potential applications in catalysis, sensing, magnetic materials, stimuli-responsive materials *etc.*<sup>1</sup> Rules based on organogelator have been usually applied to design metal-organic gels since the relationship between molecular structure and gelation is largely poorly understood. Auxiliary moieties such as cholesteryl, urea, long hydrocarbon, ether chain *etc.* are required in these gels.<sup>2</sup> To rationally design metalogels a crystal engineering approach has been developed by Dastidar and others.<sup>3</sup> In this approach, the gel fibres are extended *via* anisotropic interactions (*e.g.* self-complementary hydrogen bonding,  $\pi$ - $\pi$  interactions).<sup>3,4</sup> On the other hand, we and others recently observed a novel group of metal-organic gels based on simple rigid bridging ligands without any auxiliary moieties.<sup>5,6</sup> These rigid-ligand based gels show promising properties, *e.g.* in adsorption,<sup>5b,6c</sup> and catalysis.<sup>6b</sup>

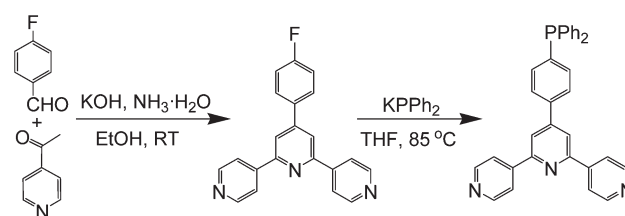
While a variety of metalogels are investigated, reports on phosphine gels are rare despite phosphines being extremely attractive in coordination chemistry<sup>7</sup> and catalysis.<sup>8</sup> Uozumi *et al.* reported a Pd(II) gel synthesised from a triphosphine with auxiliary hydrophobic alkyl-chain tether showing interesting catalytic properties.<sup>2e</sup> We obtained viscous, thixotropic silver coordination polymers in solution using a rigid bridging triphosphine, 1,3,5-tris(diphenylphosphanyl)benzene.<sup>9</sup> Herein we wish to report that metal-organic gels have been successfully obtained based on Ag(I) and rigid terpyridyl phosphine ligand, **Py2Phos**, in which terpyridine groups would generate interesting

photochemical and electronic properties.<sup>10</sup> Only AgOTf has been found to induce gelation, other than other Ag(I) salts.

Synthesis of **Py2Phos** was accomplished through the reaction sequence shown in Scheme 1. Condensation of a 2 : 1 molar ratio of 4-acetylpyridine and 4-fluorobenzaldehyde with ammonia afforded 4'-(4-fluorophenyl)-4,2':6',4''-terpyridine (**Py2F**). **Py2Phos** was synthesised from **Py2F** by reaction with potassium diphenylphosphide in THF. The <sup>31</sup>P NMR spectrum of **Py2Phos** shows a single resonance at -4.5 ppm. **Py2Phos** is a three-connecting ligand with two pyridyl N donors and one P donor, as the nitrogen atom of the central pyridine ring is not coordinated to metal centres as previously known.<sup>11</sup>

Transparent gels formed after 30 min upon simple mixing of a CHCl<sub>3</sub> solution of **Py2Phos** and a solution of AgOTf in CH<sub>3</sub>CN at a molar ratio of 1 : 1 at RT (Fig. 1). The optically transparent gels turned opaque after several days. The gel was only formed at the Ag-L = 1 : 1 stoichiometry. Using more than one equivalent of Ag<sup>+</sup>, viscous solutions formed instead. On the other hand, the use of less than one equivalent of Ag<sup>+</sup> resulted in the formation of solutions, from which a crystalline product (denoted **AgOTf**, see below) could form after 30 min. Gels formed at gelator concentrations between 0.009 and 0.020 mol L<sup>-1</sup>. NMR studies of the Ag-L = 1 : 1 mixture in CHCl<sub>3</sub>-MeCN before and after gelation revealed that the added materials (**Py2Phos** and Ag<sup>+</sup>) were all incorporated in the NMR-silent aggregates. This is consistent with previous observations that supramolecular gels yield either almost unobservable or very broad resonance signals.<sup>12</sup>

The formation of gels only occurred with AgOTf, while precipitates or solutions were obtained upon using Ag(I) salts of SbF<sub>6</sub><sup>-</sup>, ClO<sub>4</sub><sup>-</sup>, NO<sub>3</sub><sup>-</sup>, OTf<sup>-</sup>, or CF<sub>3</sub>COO<sup>-</sup>. No gel could form in the simultaneous presence of OTf<sup>-</sup> and other anions, *e.g.* OTf<sup>-</sup> : BF<sub>4</sub><sup>-</sup> = 1 : 1 or OTf<sup>-</sup> : ClO<sub>4</sub><sup>-</sup> = 1 : 1. Gels formed in various binary solvent systems of CHCl<sub>3</sub>-MeCN, CHCl<sub>3</sub>-DMF, THF-MeCN, or THF-DMF. The gels are thermo-reversible.

Scheme 1 Synthesis of **Py2Phos**.

KLGHEI of Environment and Energy Chemistry, School of Chemistry and Chemical Engineering, Sun Yat-Sen University, Guangzhou, 510275, China. E-mail: zhjyong@mail.sysu.edu.cn

<sup>†</sup> Electronic supplementary information (ESI) available: Experimental section, NMR, XPS, IR spectra and SEM, structural figures. CCDC 857926-857927. For ESI and crystallographic data in CIF or other electronic format see DOI: 10.1039/c2dt00035k

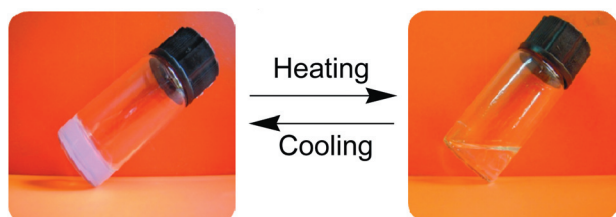


Fig. 1 Phase transition between the gel and the solution.

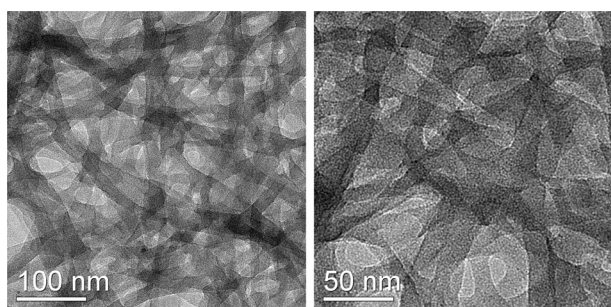


Fig. 2 TEM images of the xerogel.

Upon heating at 80 °C, gel-to-sol transition was observed, and the solutions reverted to gels upon cooling (Fig. 1). The gel-sol temperature ( $T_{\text{gel}}$ ) was determined to be 70–80 °C for the  $\text{CHCl}_3$ –MeCN gel (0.018 mol  $\text{L}^{-1}$ ) by using the “dropping ball” method in a closed vial. No single solvent was found to achieve gelation. The gels were sensitive to pH. Upon addition of acid (HOTf or HOTs), the coordinated pyridyl group of **Py2Phos** can be protonated, resulting in decomposition of the coordinated complex, which destroys the gel aggregation.

The morphology of xerogels was investigated by scanning electron microscopy (SEM) and transmission electron microscopy (TEM) (Fig. 2). The gels consist of elongated fibres with diameters of *ca.* 20 nm, which created an entangled fibrillar network. Such an extended network is typical of gels. The gel nanofibres are amorphous according to the powder XRD pattern of fresh gel, which exhibits only weak and very broad peaks.

FT-IR spectrum indicates the presence of  $\text{OTf}^-$  by the characteristic adsorption bands at 1260 and 1160  $\text{cm}^{-1}$  corresponding to the C–F and S=O vibrations, respectively. The surface analyses by XPS reveal the presence of Ag(I), as evidenced by signals at 368.9 and 374.9 eV in the Ag 3d<sub>5/2</sub> and 3d<sub>3/2</sub> region, respectively. Signals at 131.1 and 131.8 eV in the P 2P<sub>3/2</sub> and 2P<sub>1/3</sub> region, respectively, confirm attachment of the Ag(I) atoms to the PPh<sub>2</sub> groups. Thermogravimetric analysis of the xerogel shows no weight loss until *ca.* 290 °C, above which the gel network may be anticipated to collapse.

Ag(I)-based compounds are labile and readily manipulated by anions.<sup>13</sup> The gel was selectively responsive towards specific anions. Addition of salts with weakly coordinating anions such as  $[\text{Bu}_4\text{N}][\text{OTf}]$ ,  $[\text{Me}_4\text{N}][\text{NO}_3]$ ,  $[\text{Bu}_4\text{N}][\text{PF}_6]$ ,  $[\text{Bu}_4\text{N}][\text{BF}_4]$  or  $[\text{Bu}_4\text{N}][\text{ClO}_4]$  had no visible instant effect on the gel. In contrast, addition of  $[\text{Bu}_4\text{N}]\text{Br}$ ,  $[\text{Bu}_4\text{N}]\text{Cl}$ , or  $[\text{Bu}_4\text{N}]\text{OAc}$  to the gel resulted in immediate breakdown of the gel network to form a solution, which may be attributed to change of the  $\text{Ag}^+$  coordination mode induced by the anions.

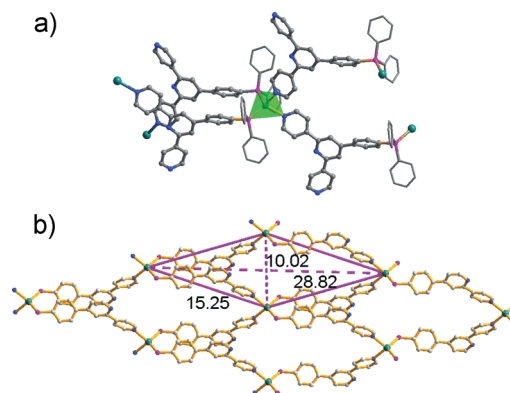
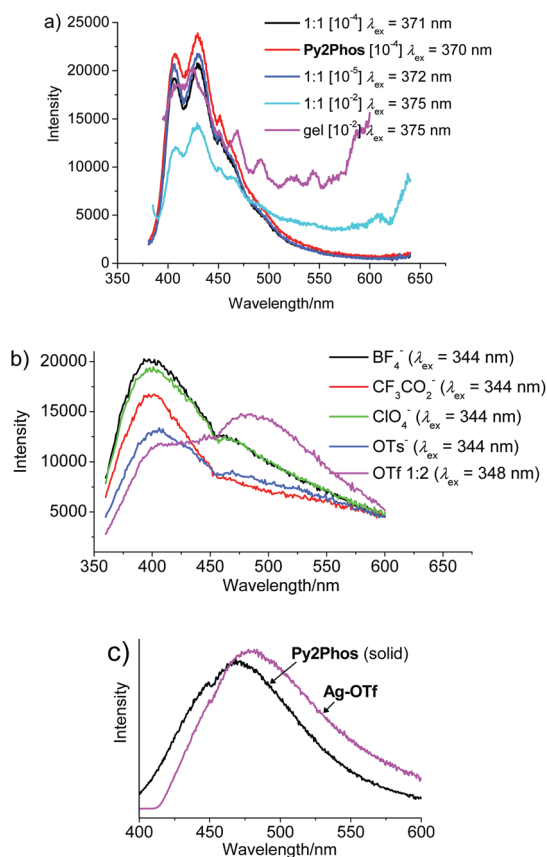


Fig. 3 X-Ray structures of **AgOTf**, (a) molecular structure showing coordination geometry of  $\text{Ag}^+$  ion, and (b) (4,4) grid network showing the size of the  $\text{Ag}_4\text{L}_4$  rhombic rings, with  $\text{OTf}^-$ , PPh<sub>2</sub> phenyl rings and uncoordinated pyridyl rings omitted for clarity.

The crystal structures of related complexes could be obtained. From the solution mixture of **Py2Phos** and **AgOTf** or **AgBF<sub>4</sub>** with a Ag–L ratio of 1 : 2, **AgOTf** ( $\text{Ag}(\text{Py2Phos})_2\text{OTf}\cdot x\text{H}_2\text{O}$ ) and **AgBF<sub>4</sub>** ( $\text{Ag}(\text{Py2Phos})_2\text{BF}_4\cdot \text{H}_2\text{O}$ ) formed. X-Ray diffraction analyses reveal that **AgOTf** and **AgBF<sub>4</sub>** are isostructural with 2D coordination polymeric structures, and only **AgOTf** is discussed here in detail. The centre  $\text{Ag}^+$  ion adopts a tetrahedral geometry and is tetracoordinate with two P donors and two pyridyl N donors from four different ligands (Fig. 3a). Each ligand binds two  $\text{Ag}^+$  ions with one P and one outer pyridyl N donor, leaving the other outer and central pyridyl N donors uncoordinated. Overall the  $\text{Ag}^+$  ions as 4-connected nodes are bridged by 2-connected ligands to form 2D grid structures of (4,4) net topology (Fig. 3b). The  $\text{Ag}\cdots\text{Ag}$  distance separated by **Py2Phos** is 15.25 Å. The rhombus grid has a size of 28.82 × 10.02 Å, with the angles being 38.4 and 141.6°, which is estimated by two diagonal  $\text{Ag}\cdots\text{Ag}$  distances and two vertex angles  $\angle\text{Ag}\cdots\text{Ag}\cdots\text{Ag}$  with the  $\text{Ag}_4\text{L}_4$  grid. The  $\text{OTf}^-$  counteranions are located in the cavities formed in a single (4,4) network. Instead  $\text{BF}_4^-$  and solvated water are located in the cavities for **AgBF<sub>4</sub>**. Three pyridyl rings of the ligand are non-planar with dihedral angles 17–30°. Intralayer  $\pi$ – $\pi$  stacking interactions exist between the parallel displaced bridging phenyl and central pyridyl rings with interplanar distances *ca.* 3.35 and 3.61 Å, respectively. The 2D networks do not interpenetrate and stack along the *c* axis in an *ABAB* sequence with an interlayer separation of *c*/2 (*ca.* 10.04 Å) via offset-face-to-face  $\pi$ – $\pi$  interactions between the central and uncoordinated pyridyl rings and edge-to-face  $\pi$ – $\pi$  interactions between phenyl rings. The phase homogeneity of **AgOTf** and **AgBF<sub>4</sub>** could be confirmed by powder XRD, the pattern of which closely matches the simulated one from the single-crystal analysis.

More information on the supramolecular organisation is provided by luminescent spectroscopy (Fig. 4). The free ligand displays a broad emission profile at the concentration of  $10^{-4}$  mol  $\text{L}^{-1}$  in  $\text{CHCl}_3$ –MeCN (*v* : *v* = 1 : 1), in which two maximum peaks can be identified at *ca.* 407 and 430 nm ( $\lambda_{\text{ex}}$  = 370 nm). For the Ag–L = 1 : 1 solutions at the concentration of  $10^{-5}$  and  $10^{-4}$  mol  $\text{L}^{-1}$  in  $\text{CHCl}_3$ –MeCN (*v* : *v* = 1 : 1), neither wavelength of maximum emission nor intensity of fluorescence



**Fig. 4** (a) Photoluminescence spectra of AgOTf/Py2Phos = 1:1 systems in solution and gel states, (b) Ag/Py2Phos = 1:1 solutions (0.0025 mol L<sup>-1</sup>) with different anions, and AgOTf/Py2Phos = 1:2 solution (*c*(Py2Phos) = 0.01 mol L<sup>-1</sup>), measured in CHCl<sub>3</sub>-MeCN (*v*:*v* = 1:1) at RT, and (c) solid-state emission spectra of Py2Phos (λ<sub>ex</sub> 360 nm) and AgOTf (λ<sub>ex</sub> 385 nm).

changes significantly. The emission is indicative of ligand-based intramolecular charge transfer (ICT) character. A structured luminescent spectrum was obtained for the Ag-L = 1:1 solution at higher concentration (10<sup>-2</sup> mol L<sup>-1</sup>, prior to gelation). The strongest emission peaks appear at the same positions to other solutions (*ca.* 407 and 430 nm excited at 375 nm) with decreased emission. It is noticeable that the emission increases as the solution starts to form gel. The gel (10<sup>-2</sup> mol L<sup>-1</sup>) exhibits similar emission characteristics upon excitation at 375 nm (Fig. 4a).

In comparison, the Ag-L = 1:2 solution shows a lower energy emission at *ca.* 480 nm with a shoulder at *ca.* 400 nm (Fig. 4b). It is attributed to π-π interactions compared with the emission of AgOTf in the solid state. The emission spectrum of AgOTf exhibits a weak broad peak at *ca.* 478 nm (λ<sub>ex</sub> = 385 nm), which undergoes a red shift from *ca.* 468 nm of the ligand (λ<sub>ex</sub> = 360 nm) attributed to coordination interactions between Py2Phos and Ag(I) ions (Fig. 4c). In addition, in the presence of other anions such as BF<sub>4</sub><sup>-</sup>, CF<sub>3</sub>CO<sub>2</sub><sup>-</sup>, ClO<sub>4</sub><sup>-</sup> and OTf<sup>-</sup>, the 1:1 solutions exhibit an emission peak at around 400 nm and a broad shoulder at 465 nm, suggesting aggregation *via* π-π interactions (Fig. 4b).

Overall, π-π interactions facilitate excimer formation and weaken light emission in solid state and the Ag-L = 1:2

solution. Upon formation of the Ag-L = 1:1 gel, the luminescent spectrum of the gel is similar to the overall profile of the ligand in dilute solution with comparable emission intensity, suggesting interesting emission enhancement in the gel state.<sup>14</sup> We would conclude that the Ag-L = 1:1 systems and gel formation significantly reduce the degree of aggregation *via* π-π interactions.

A possible formation mechanism of the gel nanofibres may be thus proposed. Py2Phos with divergent phosphorus and pyridyl donors may efficiently bridge the Ag<sup>+</sup> ions to form oligomeric or polymeric species as revealed by NMR. The Ag-L = 1:1 composition of the gel and the 1:2 composition of the crystal structures suggest that differences in coordination interactions may be important in establishing whether gelation or crystallisation occurs. Stronger Ag-P and Ag-N(pyridyl) coordination bonds are the primary forces to direct the structure and form the nanofibres, while π-π interactions between the ligands are remarkably suppressed. Especially, anions (OTf<sup>-</sup>) play a key role in formation and stabilisation of the nanofibres, which however is undefined so far.

In summary, rigid terpyridine phosphine-containing luminescent gels have been synthesised. The gel formation is dependent on metal-to-ligand ratio, anion, solvent and concentration. Ag-ligand coordination bond is crucial for the gelation by reducing π-π interactions between terpyridine groups. The gel emits blue luminescence, which emission intensity is comparable to that of the ligand in dilute solution.

## Acknowledgements

We acknowledge the NSFC (20903121 and U0934003), the NSFPG (S2011010001307), the RFDP of Higher Education of China, the Fundamental Research Funds for the Central Universities, and the 973 Program (2012CB821701) for support.

## Notes and references

- (a) M.-O. M. Piepenbrock, G. O. Lloyd, N. Clarke and J. W. Steed, *Chem. Rev.*, 2010, **110**, 1960; (b) F. Fages, *Angew. Chem., Int. Ed.*, 2006, **45**, 1680.
- (a) S.-i. Kawano, N. Fujita and S. Shinkai, *J. Am. Chem. Soc.*, 2004, **126**, 8592; (b) H.-J. Kim, J.-H. Lee and M. Lee, *Angew. Chem., Int. Ed.*, 2005, **44**, 5810; (c) A. Kishimura, T. Yamashita, K. Yamaguchi and T. Aida, *Nat. Mater.*, 2005, **4**, 546; (d) J. Liu, P. He, J. Yan, X. Fang, J. Peng, K. Liu and Y. Fang, *Adv. Mater.*, 2008, **20**, 2508; (e) Y. Pan, Y. Gao, J. Shi, L. Wang and B. Xu, *J. Mater. Chem.*, 2011, **21**, 6804; (f) Y. M. A. Yamada, Y. Maida and Y. Uozumi, *Org. Lett.*, 2006, **8**, 4259.
- P. Dastidar, *Chem. Soc. Rev.*, 2008, **37**, 2699.
- K. N. King and A. J. McNeil, *Chem. Commun.*, 2010, **46**, 3511.
- (a) Q. Wei and S. L. James, *Chem. Commun.*, 2005, 1555; (b) M. R. Lohe, M. Rose and S. Kaskel, *Chem. Commun.*, 2009, 6056; (c) S. Zhang, S. Yang, J. Lan, Y. Tang, Y. Xue and J. You, *J. Am. Chem. Soc.*, 2009, **131**, 1689; (d) S. Zhang, S. Yang, J. Lan, S. Yang and J. You, *Chem. Commun.*, 2008, 6170; (e) T. D. Hamilton, D.-K. Bucar, J. Baltrusaitis, D. R. Flanagan, Y. Li, S. Ghorai, A. V. Tivanski and L. R. MacGillivray, *J. Am. Chem. Soc.*, 2011, **133**, 3365; (f) H. Lee, S. H. Jung, W. S. Han, J. H. Moon, S. Kang, J. Y. Lee, J. H. Jung and S. Shinkai, *Chem.-Eur. J.*, 2011, **17**, 2823.
- (a) J. Zhang, S. Chen, S. Xiang, J. Huang, L. Chen and C. Y. Su, *Chem.-Eur. J.*, 2011, **17**, 2369; (b) J. Huang, L. He, J. Zhang, L. Chen and C. Y. Su, *J. Mol. Catal. A: Chem.*, 2010, **317**, 97; (c) S. Xiang, L. Li, J. Zhang, X. Tan, H. Cui, J. Shi, Y. Hu, L. Chen, C. Y. Su and S. L. James, *J. Mater. Chem.*, 2012, **22**, 1862-1867.
- (a) S. L. James, *Chem. Soc. Rev.*, 2009, **38**, 1744; (b) R. J. Puddephatt, *Chem. Soc. Rev.*, 2008, **37**, 2012; (c) R. Meijboom, R. J. Bowan and S.

- J. Berners-Price, *Coord. Chem. Rev.*, 2009, **253**, 325; (d) S. Maggini, *Coord. Chem. Rev.*, 2009, **253**, 1793.
- 8 For example see: D. S. Surry and S. L. Buchwald, *Angew. Chem., Int. Ed.*, 2008, **47**, 6338.
- 9 J. Zhang, X. Xu and S. L. James, *Chem. Commun.*, 2006, 4218.
- 10 U. Schubert, H. Hofmeier and G. R. Newkome, *Modern Terpyridine Chemistry*, Wiley-VCH, Weinheim, 2006.
- 11 For example see: E. C. Constable, G. Zhang, E. Coronado, C. E. Housecroft and M. Neuburger, *CrystEngComm*, 2010, **12**, 2139.
- 12 B. Escuder, M. Llusar and J. F. Miravet, *J. Org. Chem.*, 2006, **71**, 7747.
- 13 G. O. Lloyd and J. W. Steed, *Nat. Chem.*, 2009, **1**, 437.
- 14 (a) W. L. Leong, S. K. Batabyal, S. Kasapis and J. J. Vittal, *Chem.–Eur. J.*, 2008, **14**, 8822; (b) S. K. Batabyal, W. L. Leong and J. J. Vittal, *Langmuir*, 2010, **25**, 8451.